Diagn Interv Radiol 2023; DOI: 10.4274/dir.2023.232186

ABDOMINAL IMAGING

ORIGINAL ARTICLE

Can the Gleason score be predicted in patients with prostate cancer? A dynamic contrast-enhanced MRI, $^{(68)}$Ga-PSMA PET/CT, PSA, and PSA-density comparison study

Hüseyin Akkaya
Okan Dilek
Selim Özdemir
Zeynel Abidin Taş
İhsan Sabri Öztürk
Bozkurt Gülek

PURPOSE

The present study aims to evaluate whether perfusion parameters in prostate magnetic resonance imaging (MRI), $^{(68)}$Ga-prostate-specific membrane antigen (PSMA) positron emission tomography (PET)/computed tomography (CT), prostate-specific antigen (PSA), and PSA density can be used to predict the lesion grade in patients with prostate cancer (PCa).

METHODS

The study included a total of 137 PCa cases in which 12-quadrant transrectal ultrasound-guided prostate biopsy (TRUSBx) was performed, the Gleason score (GS) was determined, and pre-biopsy multiparametric prostate MRI and $^{(68)}$Ga-PSMA PET/CT examinations were undertaken. The patient population was evaluated in three groups according to the GS: (1) low risk; (2) intermediate risk; (3) high risk. The PSA, PSA density, pre-TRUSBx $^{(68)}$Ga-PSMA PET/CT maximum standardized uptake value (SUV_{max}), perfusion MRI parameters [maximum enhancement, maximum relative enhancement, T0 (s), time to peak (s), wash-in rate (s^{-1}), and wash-out rate (s^{-1})] were retrospectively evaluated.

RESULTS

There was no significant difference between the three groups in relation to the PSA, PSA density, and $^{(68)}$Ga-PSMA PET/CT SUV_{max} ($P > 0.05$). However, the values of maximum enhancement, maximum relative enhancement (%), T0 (s), time to peak (s), wash-in rate (s^{-1}), and wash-out rate (s^{-1}) significantly differed among the groups. A moderate positive correlation was found among the prostate volume, PSA (r = 0.490), and $^{(68)}$Ga-PSMA SUV_{max} (r = 0.322) in the patients. The wash-out rate (s^{-1}) and wash-in rate (s^{-1}) had the best diagnostic test performance (area under the curve: 89.1% and 78.4%, respectively).

CONCLUSION

No significant correlation was found between the $^{(68)}$Ga-PSMA PET/CT SUV_{max} and the GS. The wash-out rate was more successful in estimating the pretreatment GS than the $^{(68)}$Ga-PSMA PET/CT SUV_{max}.

KEYWORDS

$^{(68)}$Ga-PSMA PET/CT, prostate perfusion MRI, wash-out rate, wash-in rate, PSA, PSA density

From the Clinic of Radiology (H.A. ✉ dr.hsynakkaya@gmail.com, O.D., S.Ö., B.G.), University of Health Sciences Turkey, Adana City Training and Research Hospital, Adana, Turkey; Clinic of Pathology (Z.A.T.), University of Health Sciences Turkey, Adana City Training and Research Hospital, Adana, Turkey; Clinic of Nuclear Medicine (İ.S.Ö.), University of Health Sciences Turkey, Adana City Training and Research Hospital, Adana, Turkey.

Received 07 March 2023; revision requested 09 April 2023; last revision received 17 May 2023; accepted 22 May 2023.

Epub: 03.07.2023

Publication date: 05.09.2023

DOI: 10.4274/dir.2023.232186

The prostate-specific antigen (PSA) and digital rectal examination are the most commonly used parameters in the early diagnosis and screening of prostate cancer (PCa).[1,2] The Gleason score (GS) is globally the most widely used and accepted pathology staging criterion in determining the prostate adenocarcinoma tumor grade. This score is also associated with the prognosis of PCa.[3,4]

The Prostate Imaging–Reporting and Data System (PI-RADS) version 2.1 is based on the contrast enhancement of lesions, diffusion-weighted imaging (DWI) findings, and T2-weighted signal characteristics.[5,6] Dynamic contrast-enhanced (DCE)-magnetic resonance imaging

You may cite this article as: Akkaya H, Dilek O, Özdemir S, Taş ZA, Öztürk İS, Gülek B. Can the Gleason score be predicted in patients with prostate cancer? A dynamic contrast-enhanced MRI, $^{(68)}$Ga-PSMA PET/CT, PSA, and PSA-density comparison study. *Diagn Interv Radiol*. 2023;29(5):647-655.

(MRI) is a technique used to measure perfusion, blood flow, and tissue vascularity by examining the signal generation curve of the tissue.[7] Quantitative DCE-MRI (as seen in the Tofts model),[8] assumes two chambers representing the extravascular extracellular space and blood plasma in the examined tissue to provide absolute and, therefore, more objective values for perfusion. Semi-quantitative parameters that can be obtained using DCE-MRI can be derived from the signal intensity curve and subsequently calculated.[9,10] These parameters are the maximum enhancement, maximum relative enhancement, T0 (s), time to peak (s), wash-in rate (s^{-1}), and wash-out rate (s^{-1}).[9,11]

Molecular PCa imaging is a useful tool for systematic evaluation in tumor biology.[11] In their study, Demirci et al.[12] showed (1) a correlation between the $^{(68)}$Ga-prostate-specific membrane antigen (PSMA) maximum standardized uptake value (SUV_{max}) and the tumor grade, and (2) that intraprostatic accumulation sites may be capable of predicting clinically significant cancer, giving it the potential to serve as a target for biopsy sampling together with multi-parametric MRI (mpMRI) in selected patients. Kwan et al.[13] retrospectively compared the final pathology results of radical prostatectomy (RP) cases with positron emission tomography (PET)/computed tomography (CT) results. According to the results obtained in the study, the International Society of Urological Pathology (ISUP) grade group from the final RP was predicted using the SUV_{max}; this was also true to a lesser extent in PSA and the maximal dimension of PET-avid lesions. The SUV_{max} monotonically increased in the ISUP grade group.[13] In their retrospective study, Donato et al.[14] showed that $^{(68)}$Ga-PSMA PET/CT was successful in predicting the cancer grade after MRI and prostate biopsy.

Main points

- A moderate positive correlation was found between the prostate volume and $^{(68)}$Ga-prostate-specific membrane antigen (PSMA) maximum standardized uptake value (SUV_{max}) values.
- Prostate-specific antigen and $^{(68)}$Ga-PSMA SUV_{max} values were affected by prostate volume.
- Semi-quantitative dynamic contrast-enhanced (DCE)-magnetic resonance imaging (MRI) data were successful in predicting the extent of intraprostatic tumor lesions.
- The most valuable parameter in predicting Gleason grade among the DCE-MRI parameters was the wash-out rate, followed by the wash-in rate.

The present study aimed to investigate the performance of the PSA, PSA density, $^{(68)}$Ga-PSMA PET/CT, and perfusion MRI values as the most commonly used PCa diagnostic methods in cancer grade prediction.

Methods

Patient selection and study design

The present study was conducted in full accordance with the guidelines of the Declaration of Helsinki, revised in 2000 in Edinburgh. Approvals for the study were obtained from the Ethics Committee of University of Health Sciences Turkey, Adana City Training and Research Hospital and the Turkish Ministry of Health (2022/2115). The requirement for informed consent from the patients was waived due to the retrospective nature of the study.

In this study, a total of 207 patients with PI-RADS 4–5 lesions detected using prostate mpMRI examinations, performed between January 2018 and August 2022, were identified. Transrectal ultrasonography-guided 12-quadrant prostate biopsy (TRUSBx) was performed by urologists and interventional radiologists, and GSs were determined. Patients who underwent prostate mpMRI, $^{(68)}$Ga-PSMA PET/CT, and serum PSA examinations before biopsy were included in the study. First, PI-RADS categorization was performed for all patients included in the study; next, quantitative perfusion measurements from DCE-MRI sections of PI-RADS 4–5 lesions were made (Table 1).

The inclusion criterion was as follows: patients with a GS of ≥6 without extracapsular extension.

The exclusion criteria were as follows: (1) Patients without $^{(68)}$Ga-PSMA PET/CT or PSA examinations; (2) patients with a history of prostate surgery or pelvic radiotherapy; (3) patients with insufficient pathology result material; (4) patients without non-adenocarcinoma according to the pathology report; (5) patients with poor MRI quality; (6) patients with suspected extra-prostatic extension in mpMRI; (7) patients with unavailable biopsy results; (8) patients without pre-biopsy mpMRI (Figure 1).

A total of 137 patients met the study criteria and were eligible for evaluation.

Due to the older age of the patients and the low urooncology cooperative group performance, there were few cases of RP. Therefore, transrectal ultrasound-guided prostate biopsy results were included in the study instead of RP diagnoses.

The PSA density was obtained by dividing the PSA value by the prostate volume. In the calculation of prostate volume, the following formulas were applied: (1) ellipsoid volume = length × width × height × $\pi/6$, and (2) bullet (cylinder + half ellipsoid) volume = length × width × height × $5\pi/24$.[15,16] Depending on the shape of the lesion measured, either an ellipsoid or bullet volume measurement method was used.

The grading guidelines for PCa were issued by the ISUP, based on a consensus conference held in 2014.[17] Prostate grading was divided into five separate groups. However, in some oncology studies, certain subgroups were combined and examined as three groups according to tumor aggressiveness

Table 1. Median (min–max) values of the parameters evaluated in the study

	Median (min–max)
Age	69 (53–90)
$^{(68)}$Ga-PSMA SUV_{max}	6.72 (2.12–35.42)
PSA (μg/L)	7.71 (0.79–36.22)
PSA density (ng/mL^2)	0.17 (0.01–0.55)
Prostate volume (cm^3)	44 (14–124)
Maximum enhancement	987.32 (145.81–2646.77)
Maximum relative enhancement (%)	114.04 (48.72–211.54)
T0 (s)	30.25 (16.32–48.21)
Time to peak (s)	51.33 (24.19–234.9)
Wash-in rate (s^{-1})	9.18 (2.94–92.55)
Wash-out rate (s^{-1})	5.12 (0.15–31.26)
Gleason score (radical prostatectomy)	3 (1–7)
Gleason score (biopsy)	2 (1–7)

min, minimum; max, maximum; PSMA, prostate-specific membrane antigen; SUV_{max}, maximum standardized uptake value; PSA, prostate-specific antigen.

and recurrency risk.[4,6,9,13] In the present study, the number of patients in the three groups was determined according to the GSs to achieve homogeny: (1) GS: 3 + 3, low/very low risk (group 1); (2) GS: 3 + 4 or 4 + 3, intermediate risk (group 2); (3) GS: 8–10 high/very high risk (group 3) (Table 2).

MRI acquisition

Imaging was performed using a 3-Tesla scanner (Ingenuity; Philips Healthcare, the Netherlands) with a body-parallel array coil (SENSE Torso/cardiac coil; USA Instruments, Gainesville, FL, USA). The MRI sequences comprised essential T2-weighted images in three planes and DWIs. For contrast enhancement, 0.1 mmol/kg of gadobutrol (Gadovist, Bayer Schering Pharmaceuticals, Mississauga, Canada) was injected through the antecubital vein at a rate of 3.0 mL/s, followed by 30 mL normal saline flushing at the same injection rate. The acquisition parameters of the MRI protocols are provided in Table 3.

Acquisition of $^{(68)}$Ga-PSMA PET/CT

After the preparation and quality control of the radiotracer, all the patients received 113–384 MBq (mean: 215.3 ± 67.2 MBq, <2 nmol PSMA ligand) of $^{(68)}$Ga-PSMA-11 according to the yield of radiolabeling. Whole-body images were captured with a radiotracer using a PET/CT scanner (Ingenuity; Philips Healthcare, the Netherlands) at 40–60 minutes after injection. The patients were placed on the scanner table in a supine position, and a CT transmission scan without intravenous contrast enhancement was acquired using a low tube current (130 kVp, 48–76 mAs), 4.0 mm slice thickness, 0.6 s gantry rotation, and 6 × 3 mm collimator width. Then, PET emission scanning was performed for 3 min per bed position, with the identical transverse

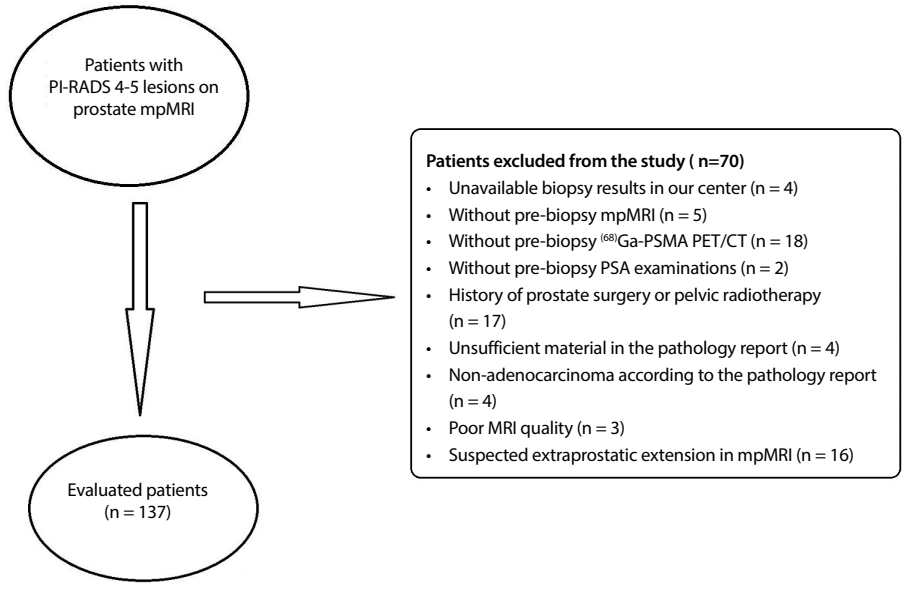

Figure 1. The initial overall number of patients, together with the number of patients included in the study, is demonstrated. The number of patients excluded from the study and exclusion criteria of the study are shown. mpMRI, multi-parametric magnetic resonance imaging; PSMA, prostate-specific membrane antigen; PET, positron emission tomography; CT, computed tomography; PI-RADS, Prostate Imaging–Reporting and Data System.

Table 2. Distribution of patients according to the Gleason score

	Frequency (n)	Percentage (%)
Group		
Gleason score, low risk	36	26.28
Gleason score, intermediate risk	50	36.50
Gleason score, high risk	51	37.22
Gleason score		
3 + 3	36	26.28
3 + 4	36	26.28
4 + 3	14	10.21
4 + 4	25	18.25
4 + 5	17	12.41
5 + 4	5	3.65
5 + 5	4	2.92

Table 3. Multiparametric examination protocol

Parameter	T2-weighted axial/coronal/sagittal	DWI axial	Pre-contrast T1 FFE axial	Dynamic contrast-enhanced T1 FFE axial	Post-contrast T1 SPIR axial
TR (msec)	3.500/3.600/4.300	4.3	10.0	5.5	524.3
TE (msec)	100/110/110	86	1.6	1.2	9.0
Slice thickness (mm)	3	3	4	4	3
Interslice gap (mm)	0.3	0.3	0	0	0
Matrix size	316 × 272/308 × 272/316 × 255 (respectively)	120 × 118	216 × 166	216 × 166	308 × 266
Flip angle (degree)	–	–	5/15	10	–
FOV (mm × mm)	220 × 220	180 × 180	300 × 300	300 × 300	220 × 220
b values (s/mm^2)	–	0, 600,1500	–	–	–
Number of slices	30/30/26	30	24	39	30
Acquisition time (minute/second)	2 min 15 sec/2 min 24 sec/2 min 25 sec	7 min 9 sec	10 sec/11 sec	4 min 13 sec	2 min 26 sec

DWI, diffusion-weighted imaging; SPIR, spectral pre-saturation with inversion recovery; FFE, fast-field echo; TR, repetition time; TE, echo time; FOV, field of view.

field of view in the caudocranial direction. The visual analysis included four-point certainty scoring (definitely negative, equivocal: probably negative, equivocal: probably positive, and definitely positive), as well as the evaluation of the anatomic site and lesion size. Semi-quantitative analysis was undertaken using the SUV_{max}. Due to the retrospective nature of the study, SUV_{max} measurements were retrospectively reproduced by the nuclear medicine specialist included in the study; the specialist who performed the measurements was blinded to all remaining information.

MRI evaluation

Lesions included in the study were primarily evaluated in DWI and T2-weighted MRI sequences according to the PI-RADS version 2.1 guidelines, and semiquantitative measurements were obtained from the perfusion sequence of the lesions with PI-RADS 4–5 scores (Figures 2, 3). The images were confirmed by the $^{(68)}$Ga-PSMA PET/CT examination. There were mismatches between the two tests of 11 patients; these patients were excluded from the study.

For the measurements, all the images obtained from the software were used. Regions of interest (ROIs) were defined as areas with an abnormal signal on MRI images and were manually drawn. The ROIs were inputted using the oval-shaped function. Using these ROIs, the time-intensity curve and time-to-peak values were automatically generated. These images were evaluated on a workstation (Intelli Space Philips, the Netherlands). The following perfusion parameters were evaluated: (1) maximum enhancement; (2) maximum relative enhancement; (3) T0 (s); (4) time to peak (s); (5) wash-in rate (s^{-1}); (6) wash-out rate (s^{-1}). Maximum relative enhancement was obtained as follows: maximum signal difference (MSD)/signal baseline (SB), where MSD is the difference between the signal intensity at its maximum and SB (Figures 2, 3). The T0 (s) was calculated as the time elapsed until the contrast agent appeared on the vessel wall. Semi-quantitative DCE-MRI was exploited to achieve the parameters of maximal enhancement, maximal relative enhancement, T0, time to peak, wash-in rate, wash-out rate, brevity of enhancement, and area under the curve (AUC). The T0 was defined as the baseline duration of the curve (sec). The time to peak (s) was defined as the time elapsed between the arterial peak enhancement and the end of the steepest portion of enhancement; the wash-in rate was determined as the maximum slope between the time of onset of contrast inflow and the time of peak intensity, and the wash-out rate was determined as the fitted line slope between the start of the wash-out and the end of the measurement. Maximum enhancement was defined as the difference between the maximum signal intensity of a pixel over all dynamics and the signal intensity of the same pixel in the reference dynamic. The relative maximum enhancement was defined as the maximum signal intensity of a pixel over all dynamics relative to the same pixel in the reference dynamic: 0% indicated the same signal intensity as the reference dynamic (%).

Statistical analysis

The data were analyzed using SPSS Statistics version 25.0 (IBM Inc. Armonk, NY, USA). Categorical measurements were summarized as numbers and percentages and continuous measurements as a median (min–max) where necessary. The Shapiro–Wilk test was used to determine whether the parameters in the study showed normal distribution, the Dunn–Bonferroni test was used to determine the source of the difference among the groups, and the Kruskal–Wallis test was used in the analysis of more than two groups of parameters that did not show normal distribution.

Fleiss' kappa (κ) was used to evaluate the agreement between TRUSBx and RP:

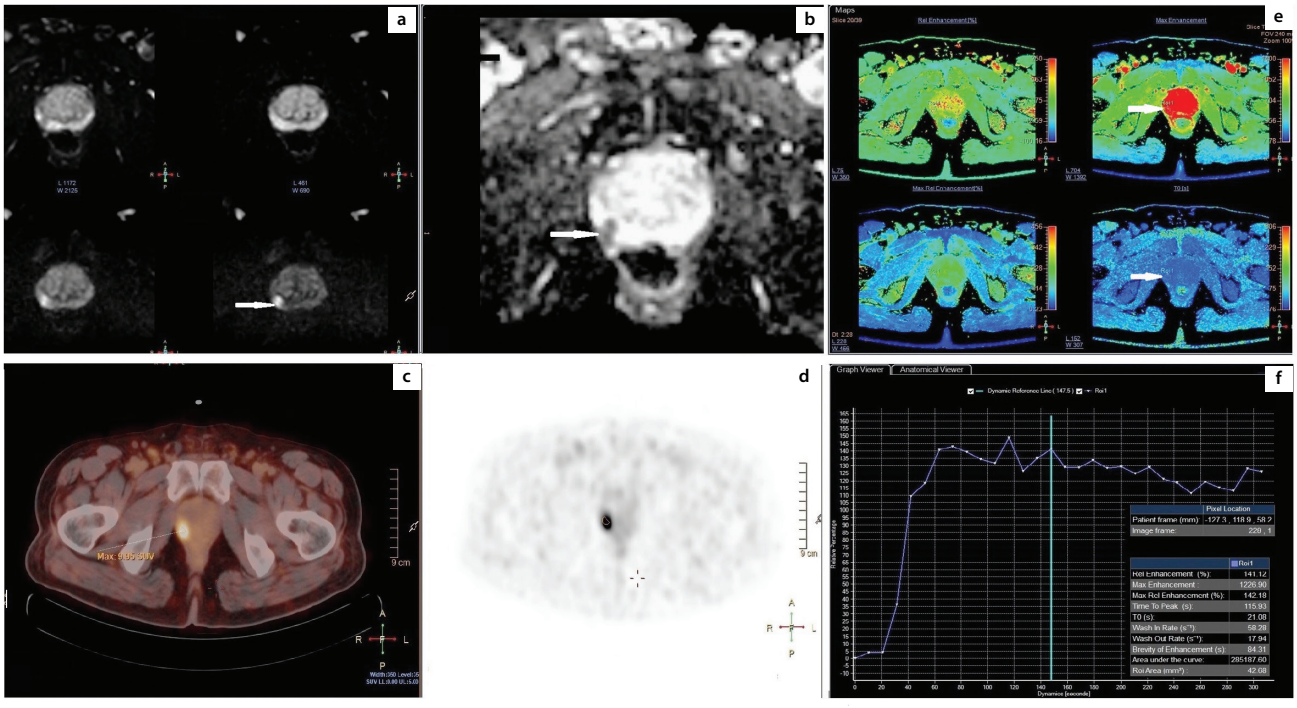

Figure 2. Peripheral zone with a PI-RADS 4 lesion, Gleason score 4 + 5, PSA: 5.72 µg/L, PSA-D: 0.23 ng/mL^2. **(a)** DWI (b = 0,600,1500 s/mm^2) shows a marked hyperintense signal (arrow) above the background. **(b)** Apparent diffusion coefficient map reveals decreased signal intensity (arrow) in the lesion. **(c, d)** $^{(68)}$Ga-PSMA-11 PET/CT images show avid uptake of radiotracer, with a SUV_{max} of 9.95. **(e, f)** DCE-MRI time-intensity curve demonstrates a decline after initial up-slope enhancement. TTP: 115.93 s^{-1}; wash-in rate; 58.28 s^{-1}, wash-out rate; 17.94 s^{-1}. PI-RADS, Prostate Imaging–Reporting and Data System; PSA, prostate-specific antigen; DWI, diffusion-weighted imaging; PSMA, prostate-specific membrane antigen; PET, positron emission tomography; CT, computed tomography; SUV_{max}, maximum standardized uptake value; DCE, dynamic contrast-enhanced; MRI, magnetic resonance imaging.

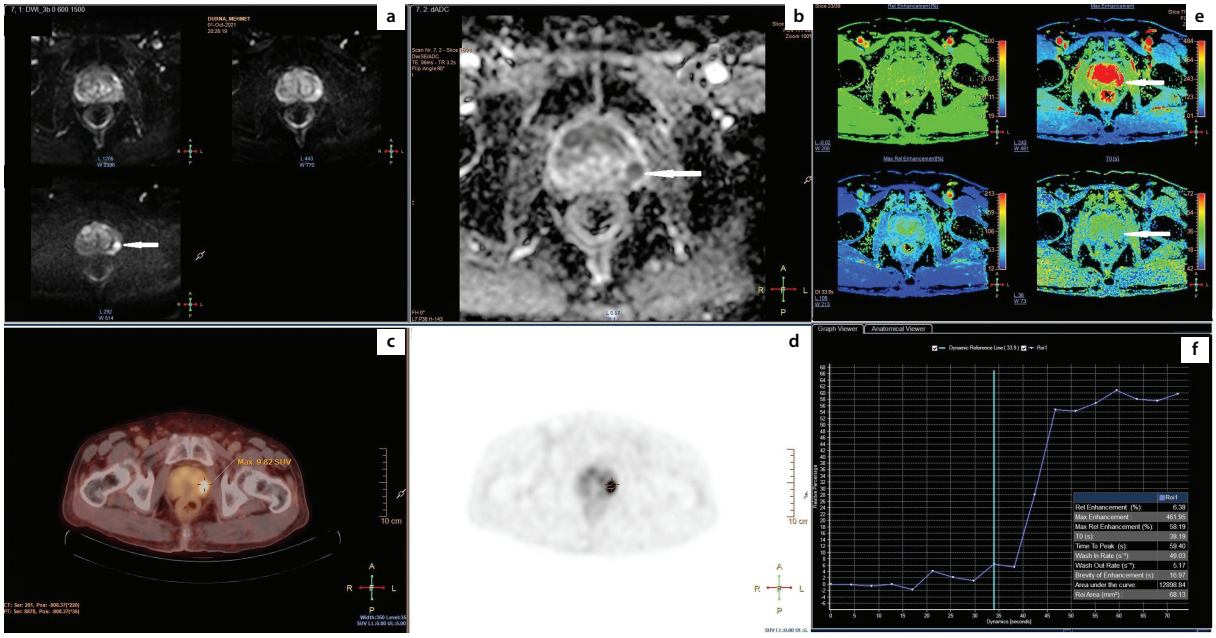

Figure 3. Peripheral zone with a PI-RADS 5 lesion, Gleason score 3 + 3, PSA: 6.84 µg/L, PSA-D: 0.21 ng/mL^2 **(a)** DWI (b = 0,600,1500 s/mm^2) shows a marked hyperintense signal (arrow) above the background. **(b)** Apparent diffusion coefficient map reveals decreased signal intensity (arrow) in the lesion. **(c, d)** $^{(68)}$Ga-PSMA-11 PET/CT images show avid uptake of radiotracer, with SUV_{max} of 9.82. **(e, f)** DCE-MRI time-intensity curve demonstrates a decline after initial up-slope enhancement. TTP: 59.4 s^{-1} ; wash in rate; 49.03 s^{-1}, wash out rate; 5.17 s^{-1}. PI-RADS, Prostate Imaging–Reporting and Data System; PSA, prostate-specific antigen; DWI, diffusion-weighted imaging; PSMA, prostate-specific membrane antigen; PET, positron emission tomography; CT, computed tomography; SUV_{max}, maximum standardized uptake value; DCE, dynamic contrast-enhanced; MRI, magnetic resonance imaging.

(1) 0.01–0.20, non-significant; (2) 0.21–0.40, weak; (3) 0.41–0.60, moderate; (4) 0.61–0.80, good; (5) 0.81–1.00, very good.[18]

The sensitivity and specificity values of the prostate volume (cm^3), maximum enhancement, maximum relative enhancement (%), T0 (s), time to peak (s), wash-in rate (s^{-1}), and wash-out rate were calculated according to the GS variable, and the cut-off values of these parameters were determined by examining the receiver operating characteristic (ROC) AUC. A ROC analysis was performed to differentiate between patients with a GS of 6 and two groups with a score of ≥7. The cut-off value was calculated according to these two groups using Youden's index. The Spearman correlation coefficient was used to determine the relationship between continuous measurements. Statistical significance was defined as $P < 0.050$.

Results

There was no significant difference among the three groups in terms of age, PSA, PSA density, and $^{(68)}$Ga-PSMA SUV_{max} values ($P > 0.05$) (Table 4); however, there were significant differences in the maximum enhancement, maximum relative enhancement (%), T0 (s), time to peak (s), wash-in rate (s^{-1}), and wash-out rate (s^{-1}) values among the groups. When the differences among the groups were further examined using the Dunn–Bonferroni test, it was observed that the patients in group 3 had a higher prostate volume (cm^3) than those in group 1. The time to peak (s) parameter had a lower mean value in group 3 compared with groups 1 and 2 ($P < 0.05$). It was observed that the patients in group 3 had higher maximum enhancement, maximum relative enhancement (%), wash-in rate (s^{-1}), and wash-out rate (s^{-1}) values than those in group 1 and group 2. The T0 (s) value was higher in group 1 than in groups 2 and 3. No significant difference was observed among the groups concerning the remaining parameters shown in Table 4 ($P > 0.05$).

The prostate volume had a moderate positive correlation with the PSA (r = 0.490) and $^{(68)}$Ga-PSMA SUV_{max} (r = 0.322) values and a weak negative correlation with PSA density (ng/mL^2) (r = –0.251) ($P < 0.001$, $P < 0.001$, and $P = 0.003$, respectively) (Table 5).

The AUC values of maximum enhancement, maximum relative enhancement (%), T0 (s), time to peak (s), wash-in rate (s^{-1}), and wash-out rate (s^{-1}), evaluated according to the GS variable, were determined as 65.3%, 65.8%, 71.9%, 72.1%, 78.4%, and 89.1%, respectively, at their optimal cut-off values. Accordingly, the wash-out rate (s^{-1}) had the best diagnostic test performance (Table 6).

The diagnostic test performances of the time to peak (s), wash-in rate (s^{-1}), and wash-out rate (s^{-1}) values, which had high AUC values, are examined in Table 7. Accordingly, it was determined that the value of the wash-out rate (s^{-1}) was stronger in predicting diagnostic test performance than the wash-in rate (s^{-1}) and the time to peak (s) ($P = 0.005$ and $P = 0.003$, respectively) (Table 7).

The multivariate ROC curves of the investigated prostate perfusion MRI parameters are shown in Figure 4 and Table 6.

The number of RP cases was small, but the Kappa analysis agreement between the GSs of TRUSBx and RP was obtained as 0.796, ($P < 0.001$) (Figure 5).

Discussion

The main purpose of this study was to compare $^{(68)}$Ga-PSMA SUV_{max}, DCE-MRI, and PSA density values, which are the most-used parameters for GS prediction in the literature. Based on the information obtained in the present study, DCE-MRI parameters, respectively, the wash-out rate, wash-in rate, and time to peak, were quite successful in predicting the GS; meanwhile, the $^{(68)}$Ga-PSMA SUV_{max} and PSA failed to predict the GS.

In the current study, no correlation was found between the PCa grade and the PSA; however, a moderate correlation was observed between the prostate volume and the PSA. Recent studies that investigated whether the addition of prostate volume to the

Table 4. Analysis of the investigated parameters according to the three patient groups, based on the Gleason score

	Group 1 (low risk) Median (min–max)	Group 2 (intermediate risk) Median (min–max)	Group 3 (high risk) Median (min–max)	*P*	Dunn-Bonferroni test
Age	69 (57–80)	68.5 (57–89)	70 (53–90)	**0.777**	
$^{(68)}$Ga-PSMA SUV_{max}	5.34 (2.18–31.84)	6.35 (2.41–35.42)	7.15 (2.12–28.91)	**0.178**	
PSA (μg/L)	6.78 (0.87–20.7)	7.40 (0.79–23.81)	8.60 (0.86–36.20)	**0.186**	
PSA density (ng/mL^2)	0.16 (0.01–0.45)	0.165 (0.01–0.44)	0.17 (0.03–0.55)	**0.717**	
Prostate volume (cm^3)	39.5 (14–122)	44 (17–116)	55 (14–124)	**0.032**	1-2; $P = 0.412$ 2-3; $P = 0.412$ 3-1; $P = 0.048$
Maximum enhancement	885.59 (145.81–1852.36)	964.38 (351.12–1785.69)	1235.23 (512.85–2646.77)	**0.001**	1-2; $P = 0.659$ 3-1; $P < 0.001$ 3-2; $P = 0.008$
Maximum relative enhancement (%)	98.49 (51.65–185.12)	111.33 (48.72–201.33)	143.12 (68.45–211.54)	**<0.001**	1-2; $P = 0.952$ 3-1; $P < 0.001$ 3-2; $P = 0.008$
T0 (s)	34.28 (20.66–48.21)	30.43 (18.31–47.28)	28.22 (16.32–43.68)	**<0.001**	1-2; $P = 0.011$ 1-3; $P < 0.001$ 2-3; $P = 0.477$
Time to peak (s)	63.03 (36.12–234.9)	53.76 (24.19–210.19)	42.19 (24.51–137.80)	**<0.001**	1-3. $P = 0.035$ 2-3; $P = 0.021$ 1-2; $P = 1.000$
Wash-in rate (s^{-1})	7.12 (2.94–85.90)	8.93 (4.26–43.19)	13.24 (6.56–92.55)	**<0.001**	1-2; $P = 1.000$ 3-1; $P = 0.001$ 3-2; $P = 0.003$
Wash-out rate (s^{-1})	3.13 (0.15–5.54)	4.62 (2.11–10.21)	8.87 (3.14–31.26)	**<0.001**	1-2; $P = 0.143$ 3-1; $P < 0.001$ 3-2; $P < 0.001$

min, minimum; max, maximum; PSA, prostate-specific antigen.

Table 5. Analysis of the correlation of prostate volume with PSA, PSA density, and $^{(68)}$Ga-PSMA SUV_{max}

	Prostate volume (cm^3)	
	r	*P*
PSA (μg/L)	0.490	**<0.001**
PSA density (ng/mL^2)	–0.251	**0.003**
$^{(68)}$Ga-PSMA SUV_{max}	0.322	**<0.001**

PSMA, prostate-specific membrane antigen; SUV_{max}, maximum standardized uptake value; PSA, prostate-specific antigen.

PSA calculation could better distinguish false from true positives showed that PSA density supplied more information for biopsy decisions than PSA alone. In tests performed on different PSA density threshold levels as predictors of PCa, a PSA density value of 0.15 remained the most accepted value for distinguishing clinically significant diseases from clinically insignificant diseases. Recent literature studies showed that PSA density had a high sensitivity in the diagnosis of PCa in small (<50 mL) and medium-sized (50–75 mL) prostates; however, the sensitivity of this parameter was significantly lower in large (>75 mL) prostates.[2,15] In the current study, the ability of PSA density to predict the GS was evaluated, and it was determined to have no significant value for this purpose. The prostate volume of patients with a high tumor grade was greater than in those with a low tumor grade, suggesting that PSA density might be misleading in PCa diagnosis.

The clinical use of $^{(68)}$Ga-PSMA PET/CT appears to have replaced CT; it also seems superior to MRI in the detection of metastatic diseases.[19] In addition, an increasing number of studies advocate that $^{(68)}$Ga-PSMA PET/CT is superior to mpMRI in detecting PCa. However, there are also studies arguing that, particularly in patients with a large prostate volume, $^{(68)}$Ga-PSMA SUV_{max} increases PSMA expression independently of the GS.[20,21] In the present study, it was observed that the prostate volume and PSMA SUV_{max} values had a moderate correlation; however, there was no correlation between GS and the PSMA SUV_{max} values of the lesions. Uprimny et al.[22] reported that the tracer uptake in a primary tumor increases with the increase in GS and PSA levels. They also analyzed the GS and SUV_{max} values obtained from biopsy samples, as in this study, but not from the final results of all-gland pathology, based on RP.[23,24] However, in an immunohistochemical study evaluating the correlation between SUV_{max} values and PSMA expression in tissue samples, it was shown that the tracer uptake was directly related to the intensity of PSMA expression. However, in the same study, it was found that the tracer uptake did not show the GS.[25] Donato et al.[14] showed that $^{(68)}$Ga-PSMA PET/CT could predict the cancer grade but was still less sensitive than prostate mpMRI and prostate biopsy. It is necessary to increase the number of histopathological examinations including correlation analysis to determine whether the number of tumor cells or tumor grade is more effective for increasing the PSMA SUV_{max}.

van Niekerk et al.[26] reported that micro-vascularity increased as the lesion grade increased in patients with PCa. DCE-MRI is an important diagnostic method in the detection of focal PCa, as it increases the accuracy of the examination for the detection and evaluation of intraprostatic tumor lesions.[27] The contribution of perfusion parameters to the detection of intraprostatic lesions has

Table 6. ROC analysis of the DCE-MRI parameters according to the Gleason score variable

	Maximum enhancement	Maximum relative enhancement (%)	T0 (s)	Time to peak (s)	Wash-in rate (s^{-1})	Wash-out rate (s^{-1})
AUC (s.e.) (95% CI)	0.653 (0.051) (0.566–0.732)	0.658 (0.051) (0.572–0.737)	0.719 (0.049) (0.636–0.792)	0.721 (0.045) (0.638–0.794)	0.784 (0.046) (0.705–0.850)	0.891 (0.028) (0.826–0.938)
Cut-off	≤1354.3	≤132.67	>32.15	>51.32	≤8.59	≤4.11
Sensitivity % (95% CI)	97.2 (85.5–99.9)	83.3 (67.2–93.6)	72.22 (54.8–85.8)	88.89 (73.9–96.9)	86.11 (70.5–95.3)	80.56 (64–91.8)
Specificity (95% CI)	27.7 (19.3–37.5)	45.54 (35.6–55.8)	72.28 (55.2–74.5)	63.37 (53.2–72.7)	73.27 (63.5–81.6)	86.14 (77.8–92.2)
PPV % (95% CI)	32.1 (29.3–35)	35.3 (30.2–40.7)	42.6 (34.7–51)	46.4 (39.5–53.4)	53.4 (44.8–61.9)	67.4 (55.4–77.6)
NPV % (95% CI)	96.4 (79.2–99.5)	88.5 (78.2–94.3)	86.8 (79.3–91.9)	94.1 (86.3–97.6)	93.7 (86.7–97.1)	92.6 (86.4–96)
P	**0.003**	**0.002**	**<0.001**	**<0.001**	**<0.001**	**<0.001**

ROC, receiver operating characteristic; DCE, dynamic contrast-enhanced; MRI, magnetic resonance imaging; AUC, area under the curve; NPV, negative predictive value; PPV, positive predictive value; CI, confidence interval.

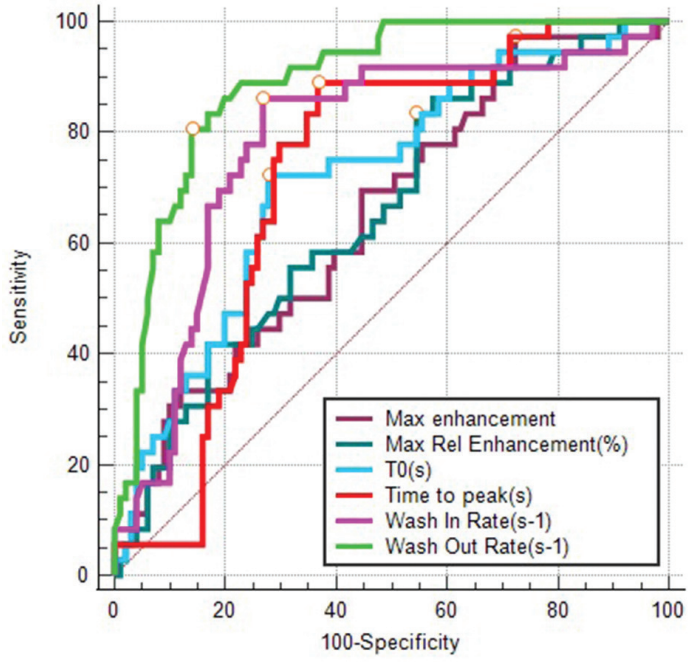

Figure 4. Multivariate ROC curve analysis of quantitative prostate perfusion parameters on MRI. ROC, receiver operating characteristic; MRI, magnetic resonance imaging.

been investigated in numerous studies.[28,29] In one of the largest series of these studies, Zhao et al.[25] demonstrated that shortening of the time to reach peak value in patients with PCa was the most sensitive DCE-MRI parameter. Ren et al.[30] indicated that DCE-MRI curves increase the ability to distinguish benign tissue from malignant prostate tissue, based on T2-weighted imaging, and that the absence of DCE-MRI causes some aggressive lesions to be missed. Boesen et al.[3] showed that the combination of measuring PSA density and performing prostate mpMRI before biopsy in patients with a GS of 7–10 increased diagnostic sensitivity and reduced the risks of unnecessary biopsy procedures.

Chen et al.[31] determined that the wash-out value had a significant correlation with GS in the evaluation of prostate tumor aggressiveness. In a similar study, Vos et al.[32] reported that quantitative parameters and semi-quantitative parameters, derived from DCE-MRI using a 3.0 T device, could assist in the evaluation of PCa aggressiveness in the peripheral zone.

In the present study, the most valuable parameter in predicting the tumor grade among the DCE-MRI parameters was the wash-out rate, followed by the wash-in rate. In tumor biology, it is known that, as the amount of non-differentiation increases, angiogenesis increases, and the microvascular bed expands.[9] Therefore, as the GS of a tumor increases, the rates of non-differentiation and angiogenesis also increase; this is represented by higher wash-out and wash-in rates in DCE-MRI evaluation.[26,32] It can be stated that the correlation between angiogenesis and the wash-out rate is more valuable than the correlation between PSMA expression and angiogenesis. However, further studies involving multimodalities are required to evaluate the correlation between angiogenesis and PSMA expression, as well as DCE-MRI parameters.

An important aspect of this study is the analysis of the lesions' multimodal characteristics. While DCE-MRI parameters reflect the microvascular nature of lesions, the SUV_{max} indicates their PSMA concentration. Thus, their combined evaluation contributes to a comprehensive assessment of tumor status and the selection of an appropriate treatment plan.

There were limitations to the present study.

(1) Kim et al.[33] reported that there was a difference in the DCE-MRI semi-quantitative parameters of lesions in peripheral and transition zones, although this did not affect the sensitivity of lesion detection. Ziayee et al.[34] determined that perfusion parameters and lesion detection rates were satisfactory for lesions in the peripheral zone but significantly reduced in those in the transition zone. In the present study, the lesions were not evaluated separately for the peripheral or transition zone; this could be considered a limitation.

Table 7. Analysis of the diagnostic test performances of wash-out rate (s^{-1}), wash-in rate (s^{-1}), and time to peak (s)

	Wash-out rate (s^{-1})	Wash-in rate (s^{-1})	Time to peak (s)	p1	p2	p3
AUC (s.e.) 95%-CI (%)	0.891 (0.028) (0.826–0.938)	0.784 (0.046) (0.705–0.850)	0.721 (0.045) (0.638–0.794)			
Cut-off	<4.11	<8.59	>51.32			
Sensitivity (%) 95%-CI (%)	80.56 (64–91.8)	86.11 (70.5–95.3)	88.89 (73.9–96.9)			
Specificity 95%-CI (%)	86.14 (77.8–92.2)	73.27 (63.5–81.6)	63.37 (53.2–72.7)	**0.005**	**0.003**	0.386
PPV 95%-CI (%)	67.4 (55.4–77.6)	53.4 (44.8–61.9)	46.4 (39.5–53.4)			
NPV 95%-CI (%)	92.6 (86.4–96)	93.7 (86.7–97.1)	94.1 (86.3–97.6)			
P	**<0.001**	**<0.001**	**<0.001**			

ROC curve test; p1, wash-out rate (s^{-1})-wash-in rate (s^{-1}); p2, wash-out rate (s^{-1})-time to peak (s); p3, wash-in rate (s^{-1})-time to peak (s). ROC, receiver operating characteristic; AUC, area under the curve; CI, confidence interval; NPV, negative predictive value; PPV, positive predictive value.

(2) In the current literature, k_{trans}, v_e, and k_{ep} calculations are used to describe DCE-MRI parameters. Although k_{trans} correlates with the initial slope (wash-in rate) of the time-intensity curve, v_e correlates with the peak height and time to peak of the time-intensity curve; k_{ep} controls the shape of the curve (reflected in the relative contributions of its independent components, K_{trans} and v_e). The authors of the present study were unable to use these parameters, since no application capable of calculating these values is available in hospital; this can be regarded as a limitation concerning the integration of the study with existing literature.

(3) In hospital, $^{(68)}$Ga-PSMA PET/CT examinations are performed on PI-RADS 4-5 lesions or in cases with a distant metastasis risk. Therefore, low PI-RADS category lesions were not included in the study in the absence of $^{(68)}$Ga-PSMA PET/CT examinations. This is accepted as a limitation due to the risk of bias.

(4) We evaluated the 3 + 4 (intermediate favorable) and 4 + 3 (intermediate unfavorable) groups as a common group in order to ensure a homogeneous distribution among the patient groups.

(5) The small number of patients who underwent RP is a limitation.

In conclusion, the semi-quantitative DCE-MRI data, especially the wash-out rate, wash-in rate, and time-to-peak values, are important diagnostic parameters for predicting the grade of intraprostatic tumor lesions. There was a moderate correlation between the prostate volume and PSMA SUV_{max} values; this may be a misleading factor for PSMA SUV_{max} prediction and GS determination.

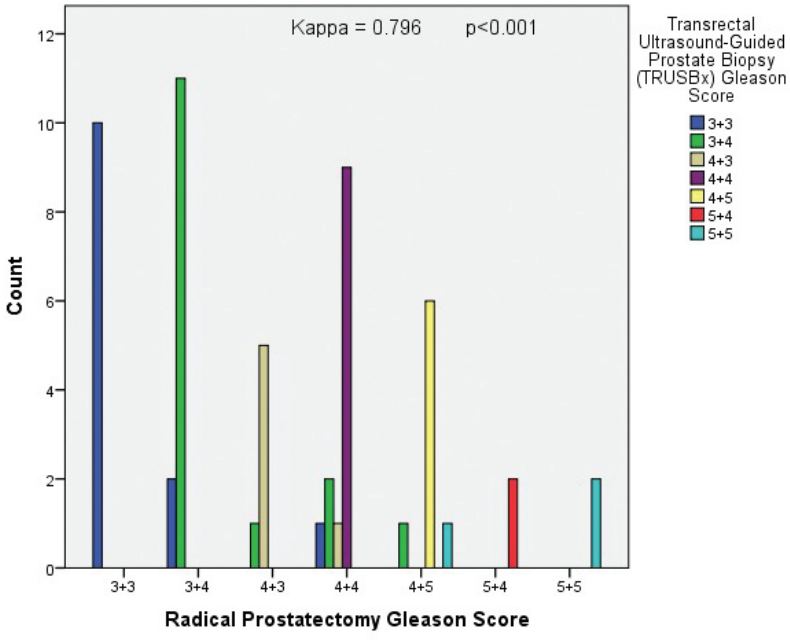

Figure 5. Kappa analysis agreement between transrectal ultrasound-guided prostate biopsy and radical prostatectomy.

Conflict of interest disclosure

The authors declared no conflicts of interest.

References

1. Turkbey B, Rosenkrantz AB, Haider MA, et al. Prostate imaging reporting and data system version 2.1: 2019 update of prostate imaging reporting and data system version 2. *Eur Urol*. 2019;76(3):340-351. [CrossRef]
2. Sauter G, Steurer S, Clauditz TS, et al. Clinical utility of quantitative Gleason grading in prostate biopsies and prostatectomy specimens. *Eur Urol*. 2016;69(4):592-598. [CrossRef]
3. Boesen L, Nørgaard N, Løgager V, et al. Prebiopsy biparametric magnetic resonance imaging combined with prostate-specific antigen density in detecting and ruling out Gleason 7-10 prostate cancer in biopsy-naïve men. *Eur Urol Oncol*. 2019;2(3):311-319. [CrossRef]
4. Godtman RA, Kollberg KS, Pihl CG, Månsson M, Hugosson J. The association between age, prostate cancer risk, and higher Gleason score in a long-term screening program: results from the Göteborg-1 Prostate Cancer Screening Trial. *Eur Urol*. 2022;82(3):311-317. [CrossRef]
5. Tan CH, Hobbs BP, Wei W, Kundra V. Dynamic contrast-enhanced MRI for the detection of prostate cancer: meta-analysis. *AJR Am J Roentgenol*. 2015;204(4):W439-W448. [CrossRef]
6. Winkel DJ, Heye TJ, Benz MR, et al. Compressed sensing radial sampling MRI of prostate perfusion: utility for detection of prostate cancer. *Radiology*. 2019;290(3):702-708. [CrossRef]
7. Tofts PS, Brix G, Buckley DL, et al. Estimating kinetic parameters from dynamic contrast-

enhanced T(1)-weighted MRI of a diffusable tracer: standardized quantities and symbols. *J Magn Reson Imaging*. 1999;10(3):223-232. [CrossRef]

8. Zhao J, Mangarova DB, Brangsch J, et al. Correlation between intraprostatic PSMA Uptake and MRI PI-RADS of [68Ga]Ga-PSMA-11 PET/MRI in patients with prostate cancer: comparison of PI-RADS version 2.0 and PI-RADS version 2.1. *Cancers (Basel)*. 2020;12(12):3523. [CrossRef]
9. Singanamalli A, Rusu M, Sparks RE, et al. Identifying in vivo DCE MRI markers associated with microvessel architecture and gleason grades of prostate cancer. *J Magn Reson Imaging*. 2016;43(1):149-158. [CrossRef]
10. Michallek F, Huisman H, Hamm B, Elezkurtaj S, Maxeiner A, Dewey M. Prediction of prostate cancer grade using fractal analysis of perfusion MRI: retrospective proof-of-principle study. *Eur Radiol*. 2022;32(5):3236-3247. [CrossRef]
11. Zhao J, Hamm B, Brenner W, Makowski MR. Lesion-to-background ratio threshold value of SUVmax of simultaneous [68Ga]Ga-PSMA-11 PET/MRI imaging in patients with prostate cancer. *Insights Imaging*. 2020;11(1):137. [CrossRef]
12. Demirci E, Kabasakal L, Şahin OE, et al. Can SUVmax values of Ga-68-PSMA PET/CT scan predict the clinically significant prostate cancer? *Nucl Med Commun*. 2019;40(1):86-91. [CrossRef]
13. Kwan TN, Spremo S, Teh AYM, McHarg D, Thangasamy I, Woo HH. Performance of Ga-68 PSMA PET/CT for diagnosis and grading of local prostate cancer. *Prostate Int*. 2021;9(2):107-112. [CrossRef]
14. Donato P, Morton A, Yaxley J, et al. 68Ga-PSMA PET/CT better characterises localised prostate cancer after MRI and transperineal prostate biopsy: Is 68Ga-PSMA PET/CT guided biopsy the future? *Eur J Nucl Med Mol Imaging*. 2020;47(8):1843-1851. [CrossRef]
15. Yusim I, Krenawi M, Mazor E, Novack V, Mabjeesh NJ. The use of prostate specific antigen density to predict clinically significant prostate cancer. *Sci Rep*. 2020;10(1):20015. [CrossRef]
16. Aminsharifi A, Howard L, Wu Y, et al. Prostate specific antigen density as a predictor of clinically significant prostate cancer when the prostate specific antigen is in the diagnostic gray zone: defining the optimum cutoff point stratified by race and body mass index. *J Urol*. 2018;200(4):758-766. [CrossRef]
17. Egevad L, Delahunt B, Srigley JR, Samaratunga H. International Society of Urological Pathology (ISUP) grading of prostate cancer - an ISUP consensus on contemporary grading. APMIS. 2016;124(6):433-435. [CrossRef]
18. Fleiss JL, Cohen J. The equivalence of weighted kappa and the intraclass correlation coefficient as measures of reliability. *Educ Psychol Meas*. 1973;33(3):613-619. [CrossRef]
19. Tulsyan S, Das CJ, Tripathi M, Seth A, Kumar R, Bal C. Comparison of 68Ga-PSMA PET/CT and multiparametric MRI for staging of high-risk prostate cancer 68Ga-PSMA PET and MRI in prostate cancer. *Nucl Med Commun*. 2017;38(12):1094-1102. [CrossRef]
20. Jochumsen MR, Sörensen J, Tolbod LP, et al. Potential synergy between PSMA uptake and tumour blood flow for prediction of human prostate cancer aggressiveness. *EJNMMI Res*. 2021;11(1):12. [CrossRef]
21. Lennartz S, Täger P, Zopfs D, et al. Lymph node assessment in prostate cancer: evaluation of iodine quantification with spectral detector CT in correlation to PSMA PET/CT. *Clin Nucl Med*. 2021;46(4):303-309. [CrossRef]
22. Uprimny C, Kroiss AS, Decristoforo C, et al. 68Ga-PSMA-11 PET/CT in primary staging of prostate cancer: PSA and Gleason score predict the intensity of tracer accumulation in the primary tumour. *Eur J Nucl Med Mol Imaging*. 2017;44(6):941-949. [CrossRef]
23. Budäus L, Leyh-Bannurah SR, Salomon G, et al. Initial experience of (68)Ga-PSMA PET/CT imaging in high-risk prostate cancer patients prior to radical prostatectomy. *Eur Urol*. 2016;69(3):393-396. [CrossRef]
24. Barbosa FG, Queiroz MA, Nunes RF, Marin JFG, Buchpiguel CA, Cerri GG. Clinical perspectives of PSMA PET/MRI for prostate cancer. *Clinics (Sao Paulo)*. 2018;73(Suppl 1):e586s. [CrossRef]
25. Zhao J, Kader A, Mangarova DB, et al. Dynamic contrast-enhanced mri of prostate lesions of simultaneous [68Ga]Ga-PSMA-11 PET/MRI: comparison between intraprostatic lesions and correlation between perfusion parameters. *Cancers (Basel)*. 2021;13(6):1404. [CrossRef]
26. van Niekerk CG, van der Laak JA, Hambrock T, et al. Correlation between dynamic contrast-enhanced MRI and quantitative histopathologic microvascular parameters in organ-confined prostate cancer. *Eur Radiol*. 2014;24(10):2597-2605. [CrossRef]
27. Winkel DJ, Heye TJ, Benz MR, et al. Compressed sensing radial sampling MRI of prostate perfusion: utility for detection of prostate cancer. *Radiology*. 2019;290(3):702-708. [CrossRef]
28. Cai W, Li F, Wang J, et al. A comparison of arterial spin labeling perfusion MRI and DCE-MRI in human prostate cancer. *NMR Biomed*. 2014;27(7):817-825. [CrossRef]
29. Sung YS, Kwon HJ, Park BW, et al. Prostate cancer detection on dynamic contrast-enhanced MRI: computer-aided diagnosis versus single perfusion parameter maps. *AJR Am J Roentgenol*. 2011;197(5):1122-1129. [CrossRef]
30. Ren J, Huan Y, Wang H, et al. Dynamic contrast-enhanced MRI of benign prostatic hyperplasia and prostatic carcinoma: correlation with angiogenesis. *Clin Radiol*. 2008;63(2):153-159. [CrossRef]
31. Chen YJ, Chu WC, Pu YS, Chueh SC, Shun CT, Tseng WY. Washout gradient in dynamic contrast-enhanced MRI is associated with tumor aggressiveness of prostate cancer. *J Magn Reson Imaging*. 2012;36(4):912-919. [CrossRef]
32. Vos EK, Litjens GJ, Kobus T, et al. Assessment of prostate cancer aggressiveness using dynamic contrast-enhanced magnetic resonance imaging at 3 T. *Eur Urol*. 2013;64(3):448-455. [CrossRef]
33. Kim JK, Hong SS, Choi YJ, et al. Wash-in rate on the basis of dynamic contrast-enhanced MRI: usefulness for prostate cancer detection and localization. *J Magn Reson Imaging*. 2005;22(5):639-646. [CrossRef]
34. Ziayee F, Mueller-Lutz A, Gross J, et al. Arterial input function for quantitative dynamic contrast-enhanced MRI to diagnose prostate cancer. *Diagn Interv Radiol*. 2022;28(2):108-114. [CrossRef]